PHYSICS AND CHEMISTRY OF SOLID STATE
V. 27, No. 2 (2026) pp. 433-439
Section: Physics

DOI: 10.15330/pcss.27.2.433-439

Vasyl Stefanyk Carpathian National University

ФІЗИКА І ХІМІЯ ТВЕРДОГО ТІЛА
Т. 27, № 2 (2026) С. 433-439
Фізико-математичні науки

PACS: 02.70.-c

ISSN 1729-4428 (Print)
ISSN 2309-8589 (Online)

I.E. Krasikova, I.V. Krasikov, V.B. Muratov, V.V. Garbuz, T.V. Khomko, O.O. Vasiliev

Microhardness and structural characteristics of hot-pressed composites AlB_{12}-Al_2O_3

Frantsevich Institute for Problems of Materials Science NASU, Kyiv, Ukraine, i.krasikova@ipms.kyiv.ua

The microhardness of ceramics in the AlB_{12}-Al_2O_3 system was studied across a wide range of component ratios. Dense composite samples were fabricated using hot pressing with nano- and submicron-sized powders of AlB_{12} and α-Al_2O_3 synthesized in-house. A nonlinear relationship between hardness and composite composition was identified, suggesting a reinforcing effect due to interfacial surface interactions. A proprietary software tool developed by the authors was employed to compute the multifractal characteristics of microstructures captured via electron microscopy. A correlation was established between the microhardness of the composites and the multifractal parameters of the interfacial structures.

Keywords: multifractality, electron microscopy, image analysis, hot pressing, composites, aluminum dodecaboride, aluminum oxide.

Received 20 July 2025; Accepted 18 June 2026, Published 30 June 2026

Introduction

The nomenclature of ceramics based on compounds of light elements has remained relatively stable in recent years. Materials such as boron carbide, titanium diboride, silicon carbide, aluminum oxide, and silicon nitride continue to be in demand across various industries. Since the development of an efficient method for producing aluminum dodecaboride (AlB_{12}) in the Frantsevich Institute for Problems of Materials Science [1], this material has transitioned from being viewed as exotic to becoming increasingly integrated into common ceramic applications due to its functional properties. These materials are characterized by exceptionally high hardness, melting points, thermal stability, elastic modulus, chemical resistance, low density, and abrasiveness. Such properties make them suitable for high-load and specialized applications, including ballistic protection for personnel and equipment.

One strategy to enhance the functional properties of ceramics is the development of composites. The introduction of secondary phases can, for example, reduce sintering temperatures, improve fracture toughness, lower thermal stresses, or improve thermal conductivity. In large-scale production, cost becomes critical. Therefore, partial replacement of expensive or scarce materials with more affordable alternatives is a rational and economically justified approach.

To date, ceramics in the AlB_{12}- Al_2O_3 system remain insufficiently explored, likely due to the limited availability of suitable raw materials. However, the method described in [1] allows efficient synthesis of AlB_{12} and produces nano-dispersed AlN as a by-product, which serves as a precursor for Al_2O_3. We developed a technology to convert $Na[Al(OH)_4]$ solution extracted from the primary product of AlB_{12} synthesis into γ- to α-Al_2O_3 nanopowder [2,3]. This has enabled a waste-free production cycle using high-quality, in-house materials with controlled particle sizes, allowing the fabrication of AlB_{12}- Al_2O_3 ceramics over a wide range of compositions.

Fractal characteristics have become increasingly prominent in modern materials science for describing the structural properties of various materials. Techniques such as electron microscopy allow for the visual assessment of particle size, morphology, degree of agglomeration, and, in some cases, the nanocrystalline structure of ceramic materials. Structural images obtained via electron or optical microscopy can provide both qualitative

descriptions and quantitative metrics. To extract such data, dedicated image analysis software is essential. These programs implement algorithms based on the most appropriate mathematical models, one of which is multifractal analysis. This method offers a mathematical framework for calculating numerical parameters that effectively characterize structural features such as fracture surfaces, porous coatings, damage zones, and grain boundaries associated with ductile-to-brittle transitions.

The theoretical foundations of these algorithms are detailed in works [4–7], which served as the basis for developing the software used in this study to calculate multifractal characteristics [8–9]. In the present research, this software was applied to investigate the multifractal properties of hot-pressed AlB_{12}– Al_2O_3 composites.

I. Methods and materials

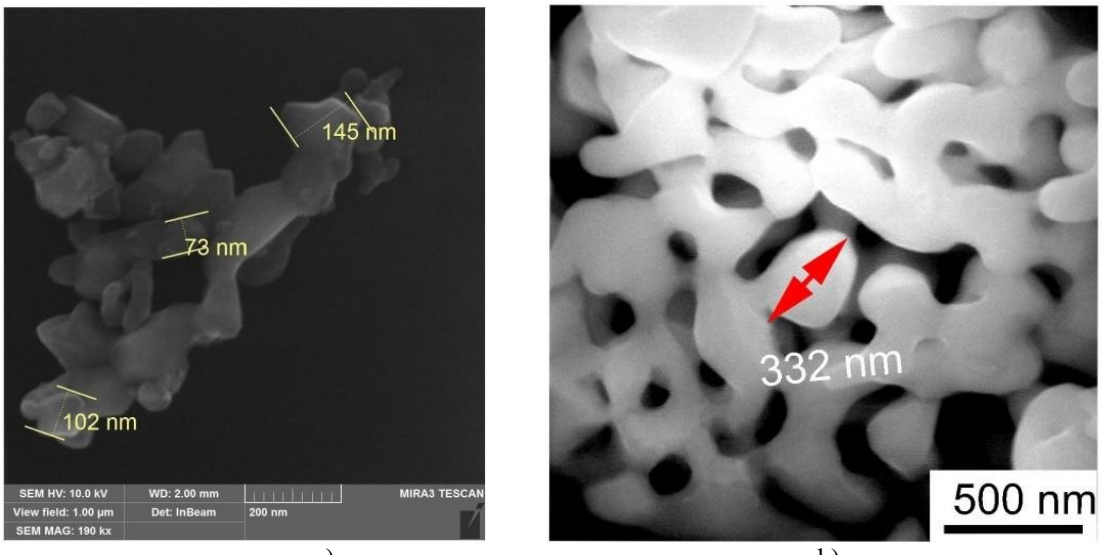
Nanocrystalline powders of aluminum oxide and aluminum dodecaboride were used to produce the ceramics. The aluminum dodecaboride α-AlB_{12}, obtained by vacuum-thermal synthesis from boron nitride and aluminum, had the following characteristics. The chemical composition of the synthesized AlB_{12} powder (wt.%): B – 81.9, Al – 17.2, B/Al – 11.9, C – 0.13, O – 0.50; lattice parameters of the tetragonal structure: $a = b = 10.1598$ Å, $c = 14.2760$ Å (no other phases were detected); the specific surface area of the batch used was 16 m^2/g, as determined by BET method. Fig. 1 shows electron microscopic images of the AlB_{12} and Al_2O_3 particles. It can be seen that the materials are of high purity and single-phase.

Note that Al_2O_3 initially precipitates as the γ-phase during the primary treatment of sodium aluminate solution $Na[Al(OH)_4]$ [2], and the figure presents α- Al_2O_3 obtained after annealing at 1300°C for three hours in air. The particle size of α- Al_2O_3 can be adjusted within certain limits by varying the temperature and annealing time.

For the study, five compositions covering a wide range of AlB_{12} and Al_2O_3 concentrations were prepared from single batches of the individual compounds. The components were mixed in ethyl alcohol using a mixer with an inclined axis of rotation. Hot pressing was carried out in graphite molds coated with boron nitride. The consolidation parameters are presented in Table 1.

After pressing, the samples were cleaned of any residual coating and ground to ensure flat and parallel surfaces. The samples had a diameter of 40 mm and a height of approximately 8 mm. Their density was determined using the hydrostatic weighing method. The measurement results are presented in Fig. 2.

It can be seen that the density of the ceramics depends linearly on their composition, increasing in proportion to the content of the Al_2O_3 oxide phase. The density of the samples–except for the composition containing 10% Al_2O_3 – is satisfactorily described by a linear relationship. This indicates the high processability of composite compaction in the AlB_{12}– Al_2O_3 system, the reliability of the established high-temperature pressure sintering parameters, and the high quality of the resulting samples (i.e., absence of under-compaction). It also suggests a consistent porosity level, estimated at no more than 2%, which, in turn, allows the influence of porosity on property variations across the full composition range to be excluded. As for the sample containing 10% Al_2O_3, which



a) b)

Fig. 1. Morphology of nano- and submicron particles of α- AlB_{12} (a) and α- Al_2O_3 (b).

Table 1.

Consolidation parameters for hot pressing of ceramic samples in the AlB_{12}– Al_2O_3 system across a wide range of compositions

Al_2O_3 content, % wt.	10	20	50	70	80
Pressing pressure, MPa	30	30	30	30	30
Sintering temperature, °C	1830	1800	1830	1800	1770
Exposure time, min.	5	16	15	15	15

exhibited a slightly lower density than predicted by the linear trend, partial under-compaction can be assumed due to the dominant content of the more refractory AlB_{12} phase.

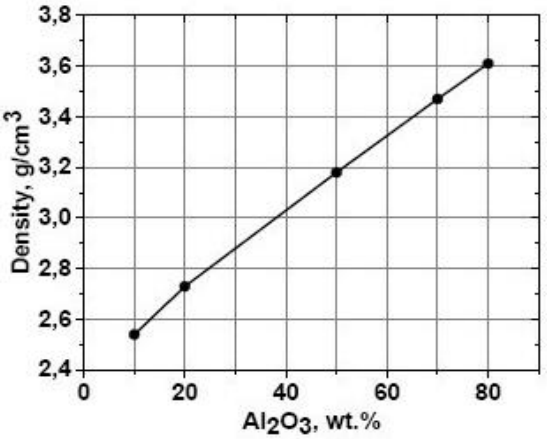


Fig. 2. Dependence of the density of AlB_{12}– Al_2O_3 ceramics on the composition.

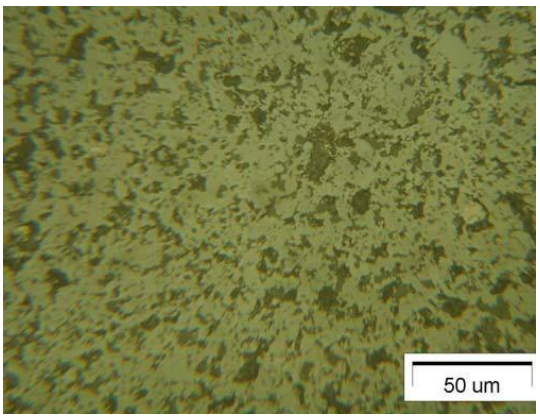
After establishing the density–composition relationship and confirming the quality of the ceramics, the samples were polished for preliminary microstructural analysis, microhardness measurements, and preparation for structural studies using fractal analysis. As an example, Fig. 3 shows the microstructure of AlB_{12}–20% Al_2O_3 and AlB_{12}–80% Al_2O_3 samples.

II. Microhardness Study

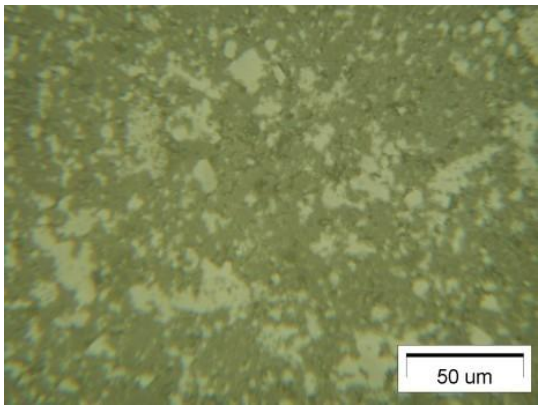
The microhardness of the obtained ceramic samples was measured using an PMT-3 microhardness tester under an indenter load of 2 N. For each composite composition, 10 independent measurements were performed. To ensure consistency throughout the study, all loading procedures and optical measurements of indentation dimensions were carried out by the same researcher.

Since the objective was to determine the overall microhardness rather than the hardness of individual phases, the indentation sites were selected at random. For illustration, Table 2 presents the initial measurement results for the AlB_{12}–50 wt.% Al_2O_3 composite. The deviation of individual measurements from the average microhardness value reflects not only random error, but primarily the intrinsic difference in microhardness between the AlB_{12} and Al_2O_3 phases.

Fig. 4 presents a graphical representation of the microhardness measurement results, including calculated confidence intervals at a standard confidence level of 0.95, based on ten independent measurements of the average values of $\bar{H}\mu$. Strictly speaking, this procedure is not statistically rigorous, as we are dealing with two distinct measurement objects – AlB_{12} and Al_2O_3 – whose areas are clearly defined. However, for illustrative purposes and improved clarity, the confidence intervals are presented in Fig. 4. It should also be noted that the microhardness of hot-pressed AlB_{12} samples is reported to be 22–23 GPa under a 5 N load [10]. As for Al_2O_3, we refer to the value of 19 GPa given in [11].



a)



b)

Fig. 3. Microstructure of hot-pressed ceramics.
a – ceramics with the AlB_{12}-20% Al_2O_3 composition;
b – ceramics with the AlB_{12}-80% Al_2O_3 composition.

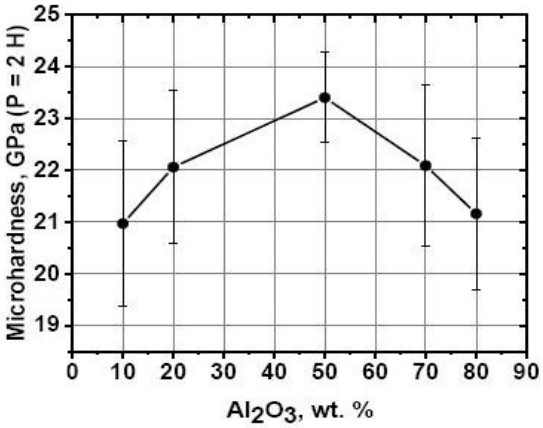


Fig. 4. Microhardness of AlB_{12}–Al_2O_3 ceramics depending on the aluminum oxide content.

In contrast to density, the microhardness of AlB_{12}–Al_2O_3 ceramics does not exhibit a straightforward dependence on composition. At 10 wt.% Al_2O_3, the average microhardness of the ceramic decreases relative to that of pure AlB_{12}. A similar effect of pronounced hardening at low additive concentrations was previously observed in the AlB_{12}–AlN system [12]. As the Al_2O_3 content increases, the microhardness of the ceramics rises, reaching an apparent maximum at 50 wt.% Al_2O_3. This

Table 2.

Microhardness of ceramics with the AlB_{12}-50% wt. Al_2O_3

#	d_1	d_2	d_{avg}	d_{avg}, μm	H_μ, GPa
1	42	41	41.5	12.45	23.92
2	43	41	42	12.6	23.35
3	41	41	41	12.3	24.51
4	45	40	42.5	12.75	22.80
5	42	40	41	12.3	24.51
6	43	40	41.5	12.45	23.92
7	45	40	42.5	12.75	22.80
8	42	40	41	12.3	24.51
9	46	40	43	12.9	22.27
10	43	41	42	12.6	23.35

$\bar{H}_\mu$ = 23.58 GPa

finding is somewhat unexpected, as the increase in Al_2O_3 content corresponds to an increase in the volume fraction of the less hard phase. The most plausible explanation is that the ceramic structure is reinforced through interparticle surface interactions.

III. Study of the structural properties of the obtained ceramics

Analysis of the microstructural images of the ceramic samples revealed no clearly defined dependence of the fractal dimension, calculated from the slope of local linear segments of the dependence of the logarithm of the generalized statistical sum on the logarithm of the box size (estimated over a finite scaling range), on the ceramic composition. As a first approximation, variations in the fractal dimension of the sample surfaces can be considered purely additive and change monotonically with the material composition (Fig. 5).

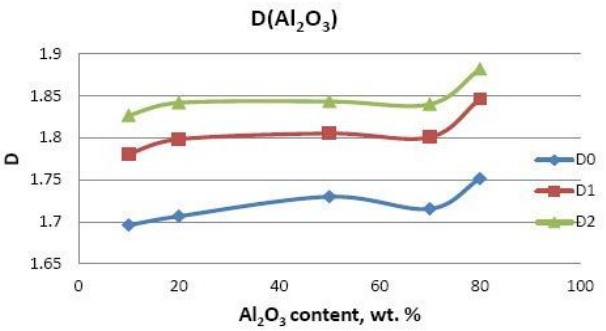


Fig. 5. Dependence of the fractal dimensions of the images of the structure of AlB_{12}– Al_2O_3 ceramics on the mass content of Al_2O_3 in the ceramic composition.

However, the situation changes significantly when analyzing the system of selected boundaries in the surface images of the studied ceramics. Examples of such boundary systems are presented in Fig. 6. As can be seen from these illustrations, the boundary detection was performed adequately, without introducing noticeable distortions. Fig. 7 presents the results of fractal dimension calculations – D_0, D_1 and D_2 – along with the corresponding microhardness values for samples with varying Al_2O_3 content in the ceramic composition.

The obtained multifractal dimensions of the boundary system demonstrate that at an aluminum oxide content of 50 wt.%, the microhardness reaches its maximum value, while the boundary system is the most developed. This conclusion follows from the observed correspondence between the extremum of the fractal dimension and the extremum of microhardness at this composition. These results confirm that microhardness is a structure-sensitive property that primarily depends on the development of the boundary system, which can be quantitatively characterized by multifractal dimensions. This finding is consistent with the earlier hypothesis that the increase in microhardness is driven by interparticle surface interactions.

Since the experimental results on the microhardness of AlB_{12}– Al_2O_3 ceramics across a broad composition range revealed distinct behavioral features – further supported by theoretical calculations of the multifractal dimensions of the boundary system – it was hypothesized that strengthening interfacial interactions are present. To verify this, the elemental distribution of the primary components of the composite ceramics at the interface between AlB_{12} and the Al_2O_3 phase was examined using electron microscopy. The microstructure of sintered AlB_{12}–50 wt.% Al_2O_3 ceramics and the results of the compositional scan are shown in Fig. 8. The image reveals that during hot pressing, the sizes of the individual phase regions (both AlB_{12} and Al_2O_3) increased significantly compared to those of the initial powders (Fig. 1). Elemental mapping of boron (a marker for AlB_{12}) and oxygen (a marker for Al_2O_3) reveals a transition zone approximately 1 μm wide at the interface between the two phases. This fully confirms the presence of interfacial interaction between AlB_{12} and Al_2O_3. As for the strengthening nature of this interaction, it is currently only indirectly supported–primarily by the observed dependence of microhardness on the ceramic composition as presented earlier in Fig. 4.

A particularly significant finding is the average microhardness of 21 GPa observed for the AlB_{12}–80 wt.% Al_2O_3 composition. The absence of a catastrophic drop in hardness for this composition indicates a strengthening effect provided by the 20 wt.% AlB_{12} content. This observation is of key importance as it opens a cost-effective way to produce the composites.

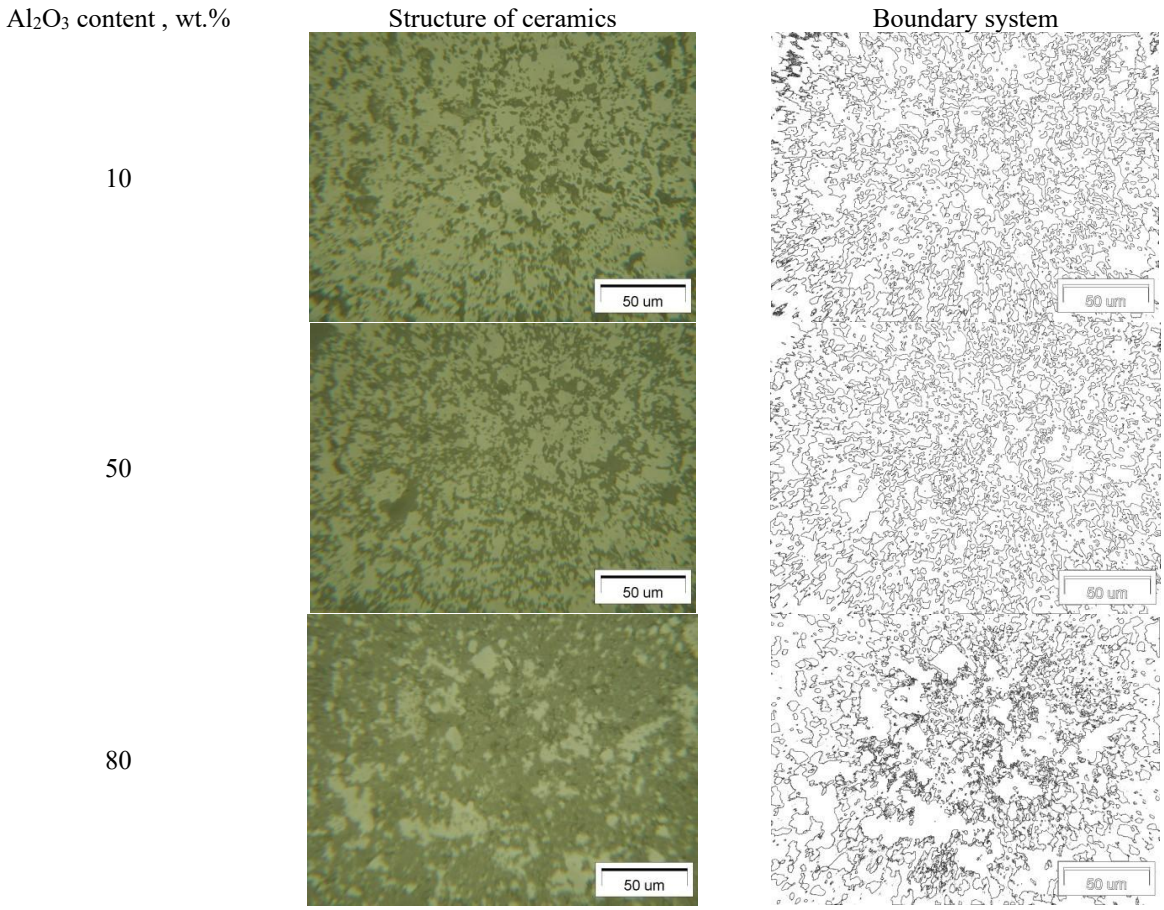


Fig. 2. Ceramic structure and systems of selected boundaries for samples with different mass content of Al_2O_3.

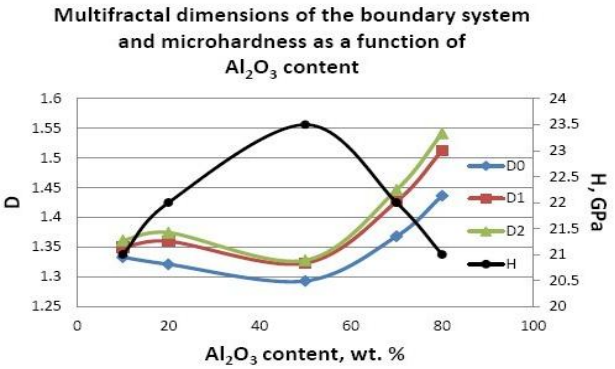


Fig.3. Fractal dimensions (D_0, D_1, D_2) of the boundary system and microhardness of samples with varying Al_2O_3 content in the ceramic composition:
$H = –19.0w^2+17.3w+19.4$ ($R^2 = 0.99$);
$D_0 = 0.82\ w^2–0.60w+1.39$ ($R^2 = 0.97$).

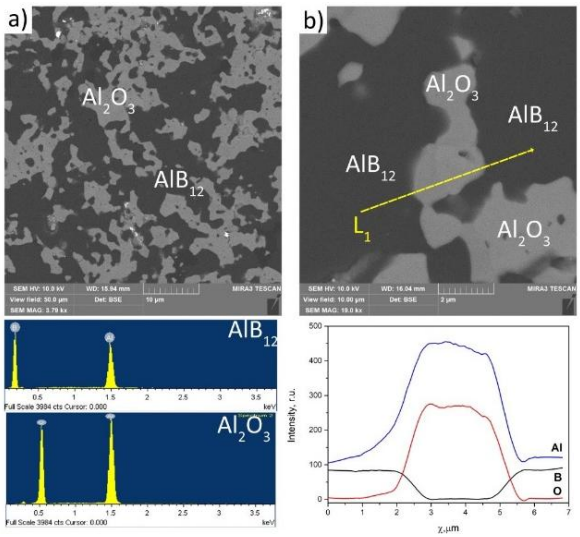


Fig. 4. Microstructure and phase boundary scanning of sintered AlB_{12}-50% Al_2O_3 ceramics.

The results obtained in this work may serve as a foundation for further research aimed at developing cost-effective methods for producing dense ceramic materials in the AlB_{12}– Al_2O_3 system with sufficient performance characteristics.

Conclusions

This study investigates the dependence of microhardness in composite ceramics of the AlB_{12}– Al_2O_3 system across a broad range of compositions. It is shown that the relationship is nonlinear, with a maximum

microhardness observed at a composition containing 50 wt.% Al_2O_3. This behavior is attributed to the strengthening effect of interfacial surface interactions. To gain a more complete understanding of the correlation between microhardness and structure in this class of composites, further investigations are recommended using smaller compositional increments of Al_2O_3.

The method developed for characterizing material structure based on the tools of fractal geometry demonstrates the potential to establish a correlation between multifractal structural parameters and the mechanical properties of composite materials.

The results obtained in this study can be used as a basis for further research into the development of cost-effective, compact materials in the AlB_{12}– Al_2O_3 system – including alloyed compositions – with adequate performance characteristics and without the need for hot pressing.

These findings clearly indicate that achieving maximum hardness in AlB_{12}– Al_2O_3 composites requires a highly developed boundary system. This qualitative parameter can be effectively monitored by calculating the fractal dimensions of the selected boundary system in microstructural images. However, the specific technological details for producing such a boundary-enhanced structure remain the subject of further investigations.

Krasikova I.E. – Candidate of Physical and Mathematical Sciences, Senior Researcher;
Krasikov I.V. – Candidate of Technical Sciences, Senior Researcher;
Muratov V.B. – Candidate of Chemical Sciences, Senior Researcher;
Garbuz V.V. – Candidate of Chemical Sciences, Senior Researcher;
Khomko T.V. – Candidate of Chemical Sciences, Senior Researcher;
Vasiliev O.O. – Candidate of Chemical Sciences, Associate Professor.

[1] Patent UA, IPC (2016.01), C01B 35/04 (2016.01). P.V.Mazur, V.B.Muratov, V.V.Garbuz, E.V.Kartuzov, O.O.Vasiliev. Method for obtaining AlB_{12} aluminum dodecaboride powder. PV — Patent for utility midel No UA107193U; filed 11/26/2015; published 25.05.2016, Bull. № 10.

[2] V.V. Garbuz, V.A. Petrova, T.A. Silinskaya, T.F.Lobunets, O.I.Bykov, V.B.Muratov, T.M.Terentyeva, L.M.Kuzmenko, O.O.Vasiliev, O.I.Olifan, T.V.Homko, *Specific surface area, cryctallite size and thermokinetic of oxide formation of γ→α-Al_2O_3 nano powders at 570-1470 K*, Surface, 12 (27), 146 (2020); https://doi.org/10.15407/Surface.2020.12.146.

[3] V.V.Garbuz, T.A.Silinskaya, T.F.Lobunets, O.I.Bykov, V.B.Muratov, T.M.Terentyeva, L.M.Kuzmenko, V.A.Petrova, O.O.Vasiliev, O.I.Olifan, T.V.Khomko, *Submicro γ-, γ'-, θ- and κ- Al_2O_3 Powders from Alkaline Waster,* Powder Metallurgy and Metal Ceramics, 61 (1-2), 498 (2023); https://doi.org/10.1007/s11106-023-00339-8.

[4] I.E. Krasikova, I.V. Krasikov, V.V. Kartuzov, *Determination of fractal characteristics of materials structure by multifractal image analysis. Computational experiment on model objects,* Mathematical models and computational experiment in materials science, 9, 79 (2007).

[5] I.E. Krasikova, V.V. Kartuzov, I.V. Krasikov, *Computer realization of the algorithm for calculating the fractal dimension of the material structure from images obtained by electron microscopy,* Mathematical models and computational experiment in materials science, 13, 82 (2011).

[6] I.E. Krasikova, V.V. Kartuzov, I.V. Krasikov *Characteristics of the computer implementation of the algorithm for calculating the fractal dimension of two-dimensional images*, Mathematical models and computational experiment in materials science, 15, 69 (2013).

[7] I.E. Krasikova, V.V. Kartuzov, I.V. Krasikov, , *Computer realization of the algorithm for calculating multifractal characteristics of material structure from two-dimensional images*, Mathematical models and computational experiment in materials science, 16, 74 (2014).

[8] I.E. Krasikova, I.V. Krasikov, V.V. Kartuzov, *Correlation of the values of fractal characteristics of the material structure from electron microscopic photographs of the surface of samples with the values of their physical and mechanical characteristics,* Electron microscopy and strength of materials, 22, 3 (2016).

[9] I.E. Krasikova, I.V. Krasikov, V.V. Kartuzov, *Determination of multifractal characteristics of images of material structures*, Scientific Notes, 57, 102 (2017).

[10] T.A.Prikhna, P.P.Barvitskyi, A.V.Maznaya, V.B.Muratov, L.N.Devin, A.V.Neshpor, V.Domnich, R.Haber, M.V.Karpets, E.V.Samus, S.N.Dub, V.E.Moshchil, *Lightweight ceramics based on aluminum dodecaboride, boron carbide and self-bonded silicon carbide,* Ceramecs International, 45, 9580 (2019); https://doi.org/10.1016/j.ceramint.2018.10.065.

[11] G.V.Samsonov, The oxide handbook. Second Edition(IFI/PLENUM - Ney York-Washington-London, 1982).

[12] I.E. Krasikova, I.V. Krasikov, V.V. Kartuzov, V.B. Muratov, A.A. Vasiliev, *Multifractal characteristics of hot-pressed composites of AlB_{12}-AlN nanopowders*, Nanosystems, nanomaterials, nanotechnologies, 18 (1), 89 (2020); https://doi.org/10.15407/nnn.18.01.089.

І.Є. Красікова, І.В. Красіков, В.Б. Муратов, В.В. Гарбуз, Т.В. Хомко, О.О. Васільєв

Мікротвердість та структурні характеристики гарячепресованих композитів AlB_{12}-Al_2O_3

Інститут проблем матеріалознавства ім. І.Францевича НАНУ, Київ, Україна, i.krasikova@ipms.kyiv.ua

Мікротвердість кераміки в системі AlB_{12}-Al_2O_3 досліджували в широкому діапазоні співвідношень компонентів. Щільні композитні зразки виготовляли за допомогою гарячого пресування з нано- та субмікронними порошками AlB_{12} та α-Al_2O_3, синтезованими власними силами. Було виявлено нелінійний зв'язок між твердістю та складом композиту, що свідчить про ефект підсилення через міжфазні взаємодії поверхонь. Для обчислення мультифрактальних характеристик мікроструктур, отриманих за допомогою електронної мікроскопії, було використано власний програмний інструмент, розроблений авторами. Було встановлено кореляцію між мікротвердістю композитів та мультифрактальними параметрами міжфазних структур.

Ключові слова: мультифрактальність, електронна мікроскопія, аналіз зображень, гаряче пресування, композити, додекаборид алюмінію, оксид алюмінію.